11-14-2022

Transition-metal ions in β-Ga_2O_3 crystals: Identification of Ni acceptors

Timothy D. Gustafson
Air Force Institute of Technology

Nancy C. Giles
Air Force Institute of Technology

Brian C. Holloway
Air Force Institute of Technology

J. Jesenovec
Washington State University

B. L. Dutton
Washington State University

See next page for additional authors

Recommended Citation

T. D. Gustafson, N. C. Giles, B. C. Holloway, J. Jesenovec, B. L. Dutton, J. S. McCloy, M. D. McCluskey, L. E. Halliburton; Transition-metal ions in β-Ga2O3 crystals: Identification of Ni acceptors. J. Appl. Phys. 14 November 2022; 132 (18): 185705. https://doi.org/10.1063/5.0126467

Authors

Timothy D. Gustafson, Nancy C. Giles, Brian C. Holloway, J. Jesenovec, B. L. Dutton, M. D. McCluskey, and Larry E. Halliburton

Journal of Applied Physics

RESEARCH ARTICLE | NOVEMBER 11 2022

Transition-metal ions in β-Ga_2O_3 crystals: Identification of Ni acceptors

T. D. Gustafson ; N. C. Giles ; B. C. Holloway; J. Jesenovec ; B. L. Dutton ; J. S. McCloy ; M. D. McCluskey ; L. E. Halliburton

J. Appl. Phys. 132, 185705 (2022)
https://doi.org/10.1063/5.0126467

Journal of Applied Physics | ARTICLE | scitation.org/journal/jap

Transition-metal ions in β-Ga_2O_3 crystals: Identification of Ni acceptors

Cite as: J. Appl. Phys. **132**, 185705 (2022); doi: 10.1063/5.0126467
Submitted: 15 September 2022 · Accepted: 19 October 2022 ·
Published Online: 11 November 2022

T. D. Gustafson,[1,a)] N. C. Giles,[1] B. C. Holloway,[1] J. Jesenovec,[2,3] B. L. Dutton,[2,3] J. S. McCloy,[2,3] M. D. McCluskey,[2,4] and L. E. Halliburton[5,a)]

AFFILIATIONS

[1]Department of Engineering Physics, Air Force Institute of Technology, Wright-Patterson Air Force Base, Ohio 45433, USA
[2]Institute of Materials Research, Washington State University, Pullman, Washington 99164, USA
[3]Materials Science and Engineering Program, Washington State University, Pullman, Washington 99164, USA
[4]Department of Physics and Astronomy, Washington State University, Pullman, Washington 99164, USA
[5]Department of Physics and Astronomy, West Virginia University, Morgantown, West Virginia 26506, USA

[a)]**Authors to whom correspondence should be addressed:** Timothy.Gustafson@protonmail.com and Larry.Halliburton@mail.wvu.edu

ABSTRACT

Transition-metal ions (Ni, Cu, and Zn) in β-Ga_2O_3 crystals form deep acceptor levels in the lower half of the bandgap. In the present study, we characterize the Ni acceptors in a Czochralski-grown crystal and find that their (0/−) level is approximately 1.40 eV above the maximum of the valence band. Both Ni^{2+} ($3d^8$) and Ni^{3+} ($3d^7$) acceptors are present in the as-grown crystal. Also present are unintentional Ir^{3+} ($5d^6$) and Ir^{4+} ($5d^5$) donors. The neutral Ni^{3+} acceptors have a low-spin S = 1/2 ground state and are easily monitored with electron paramagnetic resonance (EPR). Principal values of the g matrix for these acceptors are 2.131, 2.138, and 2.233. Although paramagnetic, the singly ionized Ni^{2+} acceptors are not seen with EPR at X band (9.4 GHz). The Ir^{4+} donors are monitored with EPR and with infrared absorption spectroscopy. Exposing the Ni-doped β-Ga_2O_3 crystal to 275 nm light at room temperature increases the concentration of Ni^{3+} ions and reduces the concentration of Ir^{4+} ions as electrons move from the acceptors to the donors. After illumination, heating the crystal above 375 °C restores the initial concentrations of the Ni^{3+} and Ir^{4+} ions. Broad optical absorption bands peaking near 303 and 442 nm are attributed to the Ni^{3+} acceptors.

I. INTRODUCTION

Transition-metal ions, with their partially filled 3d shell, are easily incorporated in β-Ga_2O_3 crystals and can often be directly monitored with electron paramagnetic resonance (EPR). These ions prefer the sixfold Ga sites and can exhibit both donor and acceptor behavior. Of the transition-metal ions, Fe has been the most studied in β-Ga_2O_3.[1–12] The $Fe^{3+/2+}$ acceptor level is 0.8 eV below the minimum of the conduction band,[1,6] and the $Fe^{4+/3+}$ donor level is 0.7 eV above the maximum of the valence band.[10] In conventional semiconductor notation, these are the (0/−) and the (+/0) levels, respectively. Chromium ions have also been extensively studied in β-Ga_2O_3 crystals, with their optical properties receiving much of the attention.[13–21] Sharp emission features appearing near 690 and 696 nm in β-Ga_2O_3 crystals are the well-known R lines from the Cr^{3+} ions. A value for the (0/−) acceptor level of Cr has not been experimentally established. Recently, Cu acceptors occupying sixfold Ga sites have been investigated in β-Ga_2O_3 crystals.[22–24] Neutral Cu^{3+} acceptors have an S = 1 EPR spectrum and are responsible for intense optical absorption bands in the visible and near-ultraviolet regions. The (0/−) level of the Cu acceptors is 1.27 eV above the maximum of the valence band.[23] Additional EPR studies of transition-metal ions in β-Ga_2O_3 have focused on Ti, Mn, and Co.[25–27]

In the present paper, we use EPR to identify and characterize Ni acceptors in a doped β-Ga_2O_3 crystal. The EPR spectra show that the Ni^{3+} ($3d^7$) acceptors have a low-spin (S = 1/2) ground state, with six d electrons in the three t_{2g} orbitals (↑↓ ↑↓ ↑↓) and one unpaired d electron in an e_g orbital (↑). This deviation from Hund's rule for the d electrons is a result of a strong crystal field

(i.e., the crystal field is greater than the exchange energy that tends to align the spins parallel).[28,29] An exposure at room temperature to 275 nm light converts Ni^{2+} to Ni^{3+} and converts Ir^{4+} to Ir^{3+}. Monitoring the subsequent thermal decay of the photoinduced neutral Ni^{3+} acceptors when heated above room temperature allows us to determine a thermal activation energy and, thus, a value for the (0/−) level. In addition to a fundamental interest in Ni as a dopant, we note that this metal is widely used to form β-Ga_2O_3 Schottky-barrier diodes. Recent reports have suggested Ni will diffuse into the semiconductor and produce a new interfacial compound that, upon annealing, improves the interface quality by reducing the trap-state density.[30,31]

Our study of Ni in β-Ga_2O_3 has greatly benefited from the much earlier work on Ni^{2+} and Ni^{3+} ions in α-Al_2O_3 crystals, a material similar to β-Ga_2O_3 except for a wider bandgap. Geschwind and Remeika[28] showed that Ni^{3+} ions replace Al^{3+} ions and have a low-spin $S = 1/2$ ground state. Above 50 K, they observed a single isotropic EPR line with $g = 2.146$. In an extension of this work, Shen and Estle[32] showed that the angular dependence of the Ni^{3+} ions observed at 1.2 K is caused by a dynamic Jahn–Teller effect. According to Müller and Günthard[33] and Tippins,[34] the charge-transfer optical absorption bands from Ni^{3+} ions peak near 280 and 400 nm. Turning to the divalent charge state, Marshall *et al.*[35] described the strongly angular dependent $S = 1$ EPR spectrum of the Ni^{2+} ions in α-Al_2O_3 and Müller and Günthard[33] reported an absorption band from Ni^{2+} ions that peaks near 400 nm in α-Al_2O_3. An EPR signal from Ni^{2+} ions is not observed in the present study of β-Ga_2O_3 because the crystal-field-splitting parameter D in the spin-Hamiltonian ($H = \beta \mathbf{S}\bullet\mathbf{g}\bullet\mathbf{B} + \mathbf{S}\bullet\mathbf{D}\bullet\mathbf{S}$) is greater than the energy of the microwave photons.

II. EXPERIMENTAL DETAILS

A Ni-doped β-Ga_2O_3 crystal was grown at Washington State University by the Czochralski (CZ) method.[24,36,37] An iridium crucible, radio frequency heating, and a controlled O_2 atmosphere were used. The Ni doping level in the starting materials was 0.25 at. %, and the pulling rate was approximately 2 mm/h. A small rectangular-shaped sample, with approximate dimensions of $1 \times 2 \times 2\ mm^3$, was cut from the larger boule for use in the present investigation. The edges of this sample were along the *a*, *b*, and *c* directions, respectively. Because the distribution of dopants and impurities can be nonuniform in a boule, all the experimental results presented in this paper were taken from one sample. Additional information about the growth of β-Ga_2O_3 crystals at Washington State University and the concentrations and distribution of dopants and impurities in these crystals can be found in Ref. 38.

The EPR spectra were obtained with a Bruker EMX spectrometer and a cylindrical TM_{110} resonator (the microwave frequency was 9.39 GHz). An Oxford Instruments ESR-900 helium-gas flow system controlled the sample temperature and a Bruker NMR gaussmeter provided corrections for the small difference in the magnetic field at the sample and the spectrometer's Hall sensor. In addition to the Ni^{3+} ions, EPR verified that unintentional Ir^{4+}, Cu^{2+}, and Fe^{3+} ions were present in the as-grown crystal. Approximate concentrations of these ions were obtained by comparing their spectra (intensities, linewidths, and number of lines) to a Bruker weak-pitch EPR standard sample. A 275 nm LED (Thorlabs Model M275L4), with an output power of 45 mW, was used to convert Ni^{2+} ions to Ni^{3+} ions. Infrared absorption spectra were obtained with a ThermoScientific Nicolet 8700 FTIR spectrometer. A white-light (QTH) source, a CaF_2 beam splitter, a DTGS detector, and an ultrabroadband fused-silica wire-grid polarizer were used. Absorption spectra in the visible and near ultraviolet were taken with a Cary 5000 spectrophotometer.

The β-Ga_2O_3 crystals have a monoclinic structure described by space group C2/m (C_{2h}^3). Lattice constants at 273 K are $a = 12.214$ Å, $b = 3.0371$ Å, $c = 5.7981$ Å, and $\beta = 103.83°$.[39,40] Following the usual convention, the *b* direction is perpendicular to the mirror plane. The angle between the *a* and *c* axes is β and the c^* direction is defined to be perpendicular to the *a*–*b* plane. Tetrahedral and octahedral Ga sites in the crystal are labeled Ga(1) and Ga(2), respectively. Oxygen ions occupy three crystallographically inequivalent sites in the crystal, labeled O(I), O(II), and O(III), and are distinguished by the number and types of nearest Ga neighbors.[41] The low-spin Ni^{3+} ions are slightly smaller than the Ga^{3+} ions. Their effective ionic radii at sixfold coordinated sites are 56 and 62 pm, respectively.[42] The effective ionic radius of the larger Ni^{2+} ions at a sixfold site is 69 pm.

III. EPR SPECTRUM FROM Ni^{3+} ACCEPTORS

Figure 1(a) shows the EPR spectrum taken from an as-grown Ni-doped β-Ga_2O_3 crystal. These data were obtained at 100 K,

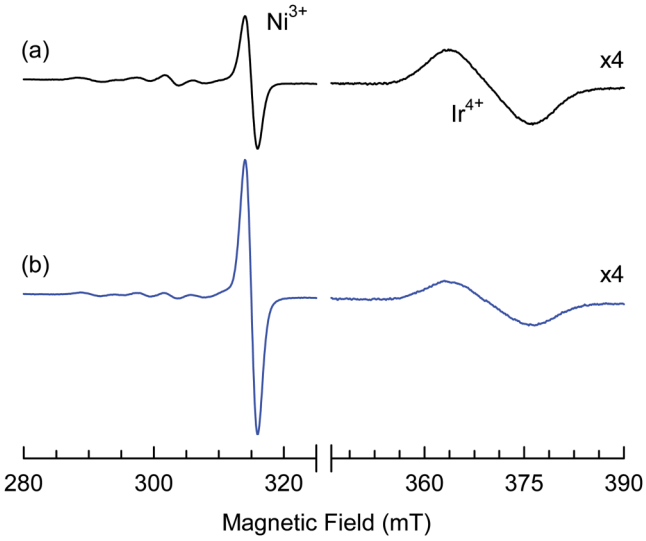

FIG. 1. EPR spectra from Ni^{3+} acceptors and Ir^{4+} donors in a Ni-doped β-Ga_2O_3 crystal. Both spectra were taken at 100 K with a microwave frequency of 9.3905 GHz. The slowly varying (static) magnetic field was along the *b* direction, and the microwave magnetic field was along the *a* direction. Intensities of the Ir^{4+} spectra have been increased by a factor of 4. (a) Before exposure to 275 nm light. (b) After an exposure to 275 nm light for 2 min while being held at room temperature.

with the magnetic field along the *b* direction and a microwave frequency of 9.3905 GHz. The prominent line at 315.0 mT is assigned to Ni^{3+} ions at octahedral Ga(2) sites and the much broader, and less intense, line at 370.5 mT is due to Ir^{4+} ions, also at Ga(2) sites. Lenyk *et al.*[43] have previously used EPR and infrared absorption to characterize Ir^{4+} ions in β-Ga_2O_3. The Ni^{3+} and Ir^{4+} (acceptor and donor) concentrations in Fig. 1(a) are 0.54×10^{19} and 2.32×10^{19} cm^{-3}, respectively. Much of the difference in these concentrations is explained by the presence of unseen Ni^{2+} ions. [Note: Because of the large anisotropy in the g matrix of the Ir^{4+} ions, the intensity of the Ir^{4+} EPR signal when the static magnetic field is along the *b* direction depends strongly on whether the microwave magnetic field in the resonator is along the *a* or *c** direction.] Weaker signals from Cu^{2+}(A) and Cu^{2+}(B) ions[23] and Fe^{3+} ions[44] are present in Fig. 1(a) in the magnetic field region slightly below the Ni^{3+} signal. The concentration of Cu^{2+}(B) ions is nearly a factor of 10 greater than the concentration of Cu^{2+}(A) ions. In the as-grown crystal, the combined concentrations of the Cu^{2+}(A) and Cu^{2+}(B) ions and the concentration of the Fe^{3+} ions are approximately a factor of 10 and a factor of 15 lower, respectively, than the Ir^{4+} concentration.

After taking the spectrum in Fig. 1(a), the crystal was warmed to room temperature and exposed to 275 nm light for 2 min while being held at this higher temperature. The crystal was then returned to 100 K, and the spectrum in Fig. 1(b) was taken. These spectra in Figs. 1(a) and 1(b) were obtained with identical spectrometer settings and, thus, can be directly compared. In each spectrum, the Ir^{4+} signals have been increased by a factor of 4. The exposure at room temperature to 275 nm light increased the intensity of the Ni^{3+} signal and decreased the intensity of the Ir^{4+} signal. Their concentrations in Fig. 1(b), after the exposure to 275 nm light at room temperature, are 1.32×10^{19} and 1.60×10^{19} cm^{-3}, respectively. The Cu^{2+} and Fe^{3+} signals, with smaller initial intensities, both decreased during exposure to the 275 nm light. The concentration of Cu^{2+} (B) ions changed from 2.2×10^{18} to 1.5×10^{18} cm^{-3}, and the concentration of Fe^{3+} ions changed from 1.5×10^{18} to 0.9×10^{18} cm^{-3}.

The angular dependence of the Ni^{3+} EPR spectrum is shown in Fig. 2. Data were obtained in 10° steps as the direction of the static magnetic field was rotated in the *a*–*b*, *b*–*c**, and *c**–*a* planes. The absence of fine-structure in the angular dependence verifies that the Ni^{3+} (d^7) ions in β-Ga_2O_3 have a low-spin S = 1/2 ground state. Also, the observation of a single line in each plane provides information about the principal-axis directions of the g matrix. As described in the recent EPR study of Ir^{4+} ions in β-Ga_2O_3,[43] the monoclinic C2/m space group permits a defect located at sixfold Ga(2) sites to have two different, but crystallographically equivalent, orientations of the principal axes of its g matrix. For the Ni^{3+} ions, the lack of splitting in the three planes in Fig. 2 indicates that the two orientations are not resolved and, thus, the principal axes of the g matrix must be close to the *a*, *b*, and *c** directions.

The angular dependence in Fig. 2 is described by a spin Hamiltonian containing only an electron Zeeman term ($H = \beta \mathbf{S} \bullet \mathbf{g} \bullet \mathbf{B}$). We write this spin-Hamiltonian as a 2×2 matrix and use a least-squares fitting program to determine the three principal values of the g matrix. The 27 discrete points in Fig. 2, along with their corresponding microwave frequencies, were used as input data and the energy eigenvalues of the matrix were repeatedly calculated as the g-matrix parameters were systematically varied. At each step of the fitting process, the predicted line positions were compared to the measured positions. Best-fit values for the three principal g values are given in Table I. The solid curves in Fig. 2 were generated using these final parameters. Our g values for the Ni^{3+} ions in β-Ga_2O_3 crystals are close to those reported for Ni^{3+} ions in α-Al_2O_2.[28,32]

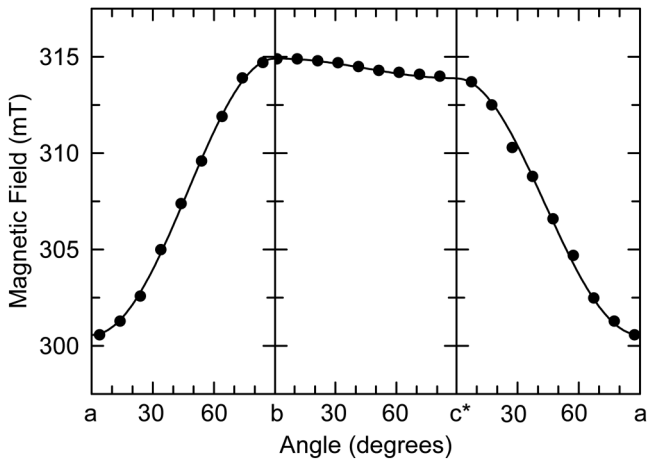

FIG. 2. Angular dependence of the EPR spectrum from Ni^{3+} ions. The direction of the magnetic field is rotated in three planes, from *a* to *b*, *b* to *c**, and *c** to *a*. Discrete points are from the experiment. The solid lines were generated using the parameters in Table I.

IV. (0/−) LEVEL OF Ni ACCEPTORS

As shown in Fig. 1, exposure to 275 nm light at room temperature increases the concentration of Ni^{3+} ions and decreases the concentration of Ir^{4+} ions. Subsequent heating in the dark restores their initial concentrations. The decay of the Ni^{3+} ions and the recovery of the Ir^{4+} ions were separately monitored with EPR and infrared absorption during a series of annealing steps above room temperature. These results are shown in Figs. 3 and 4. The Ni-doped crystal was initially exposed to 275 nm light at room temperature for 2 min. Then, after removing the light, the crystal was heated in 25 °C steps from 100 to 450 °C. The crystal was held at each higher temperature for 2 min and, after each step, an EPR spectrum of the Ni^{3+} ions was taken at 100 K and an

TABLE I. Spin-Hamiltonian parameters for Ni^{3+} ions in β-Ga_2O_3. Uncertainties are estimated to be ±0.002 for the principal g values and ±3° for the directions.

	Principal values	Principal-axis directions
g matrix		
g_1	2.131	*b*
g_2	2.138	*c**
g_3	2.233	*a*

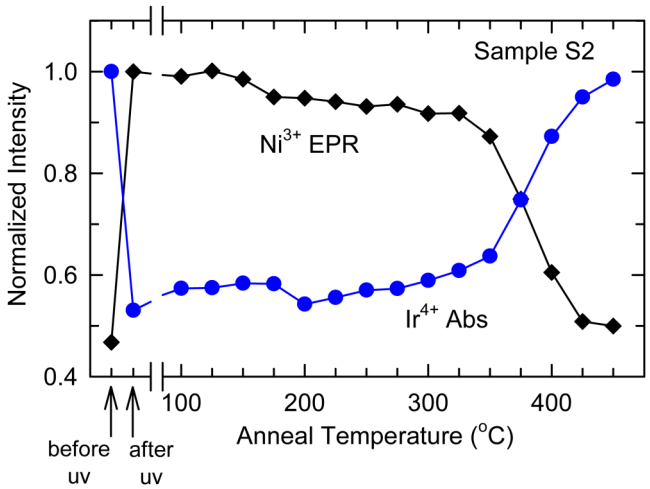

FIG. 3. Thermal decay of neutral Ni^{3+} acceptors and thermal recovery of singly ionized Ir^{4+} donors in a Ni-doped β-Ga_2O_3 crystal after an exposure to 275 nm light at room temperature. The EPR spectrum of the Ni^{3+} acceptors is monitored at 100 K, and the infrared absorption spectrum of the Ir^{4+} donors is monitored at room temperature.

infrared absorption spectrum of the Ir^{4+} ions was taken at room temperature. The Ir^{4+} infrared absorption band at 5153 cm^{-1} was monitored (light propagated along the *a* direction with E||*b*). Figure 4 shows the Ir^{4+} absorption band before and after the exposure to 275 nm light and at selected temperatures in the region where recovery occurs.

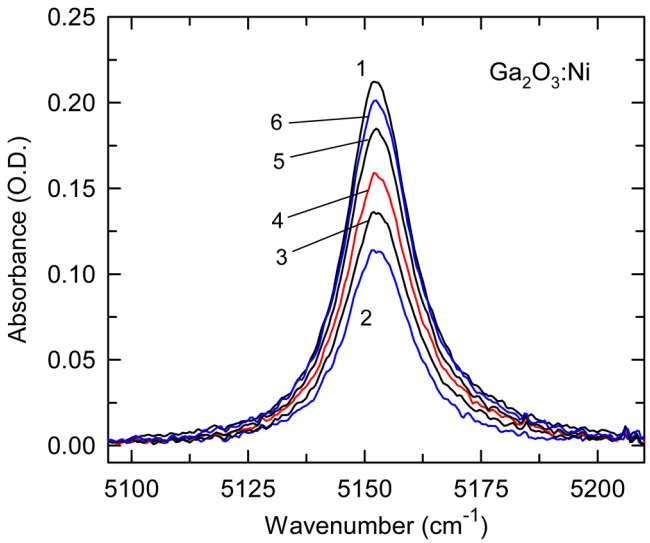

FIG. 4. Infrared absorption spectra, taken at room temperature, from Ir^{4+} ions in a Ni-doped β-Ga_2O_3 crystal. Spectrum 1 was taken before exposure to 275 nm light. Spectrum 2 was taken after exposure to 275 nm light. Spectra 3, 4, 5, and 6 were taken after heating to 350, 375, 400, and 425 °C, respectively.

In Fig. 3, the thermal decay of the photoinduced Ni^{3+} ions occurs between 325 and 425 °C. We suggest that the responsible mechanism is the thermal excitation of electrons from the valence band to the neutral Ni^{3+} acceptors, with holes left in the valence band converting the Ir^{3+} ions formed by the light back to Ir^{4+} ions. An alternative explanation where an electron is thermally excited from the Ir^{3+} ions to the conduction band can be eliminated since the $Ir^{3+/4+}$ level is near midgap[8,45] and temperatures above 750 °C would be required for thermal excitation of the electrons to the conduction band. An estimate of the activation energy describing the thermal decay of the neutral Ni^{3+} acceptors is obtained by using the approximation $E \approx 25\,kT_m$.[46,47] T_m is the temperature where half of the Ni^{3+} ions have decayed. A value of 375 °C (or 648 K) for T_m from Fig. 3 gives an activation energy of 1.40 eV for the Ni acceptors and places the (0/−) level 1.40 eV above the maximum of the valence band. The uncertainty in this value of E is estimated to be ±0.10 eV.

The relationship $E \approx 25\,kT_m$ can also be used to obtain approximate activation energies from deep-level transient spectroscopy (DLTS) data. Here, T_m would correspond to the temperature of the DLTS peak. The $Fe^{3+/2+}$ level in β-Ga_2O_3, better known as the E2 level, provides an example of the usefulness of this approximation. Ingebrigtsen *et al.*[1] found that the DLTS peak for the $Fe^{3+/2+}$ acceptor level appears at 354 K. Using this value of T_m in the 25 kT approximation for E gives an activation energy of 0.763 eV, which is very close to the value of 0.78 eV that these investigators[1] obtained from a more detailed analysis.

Table II lists experimental values for the (0/−) levels of four acceptors in β-Ga_2O_3 crystals. These results for the Mg, Zn, Cu, and Ni acceptors were obtained by using EPR to directly monitor the thermal decay of their photoinduced neutral charge states. The distinct advantage of using EPR for this purpose is the unambiguous identification of the specific acceptor being monitored, through unique g values and resolved hyperfine structure. Also, the fortuitous position of the $Ir^{3+/4+}$ donor level near midgap helps when interpreting results. Values of (0/−) are included for Zn acceptors at the tetrahedral Ga(1) and octahedral Ga(2) sites. The other three acceptors in Table II are at the Ga(2) sites. For the neutral Mg and Zn acceptors, the hole is localized on an adjacent oxygen ion in the form of a small polaron.[41,48–51] In contrast, the

TABLE II. Experimental values, obtained from EPR, for the (0/−) levels of acceptors in β-Ga_2O_3 crystals. These are the positions above the valence band. The results are given for Zn acceptors on the tetrahedral Ga(1) site and the octahedral Ga(2) site. The Cu value is for the isolated Cu(A) acceptors reported in Ref. 23.

Acceptor	(0/−) level (eV)	Reference
Mg	0.65	51
$Zn_{Ga(1)}$	0.78	41
$Zn_{Ga(2)}$	0.65	41
Cu	1.27	23
Ni	1.40	Present work

deeper neutral Cu and Ni acceptors have the hole localized in a 3d orbital within the ion.[23]

Support for the method used to obtain the acceptor values in Table II is provided by a recent experimental study of the electrical properties of Zn-doped Ga_2O_3 thin films.[52] Hall effect measurements by these investigators indicate that the Zn-related acceptor-level ionization energy is 0.77 eV above the valence band maximum, in close agreement with the EPR results in Table II. We note that computational studies often predict very different values for (0/−) levels. For example, density functional theory (DFT) calculations, using the Heyd, Scuseria, and Ernzerhof (HSE) hybrid functional, place the (0/−) levels of the Zn_{Ga1} and Zn_{Ga2} acceptors more than 1.2 eV above the valence band maximum.[36,53] In an informative DFT study of acceptors in β-Ga_2O_3, Kyrtsos *et al.*[54] found that the PBE and HSE formalisms gave significantly different (0/−) values. For Zn acceptors, the generalized gradient approximation (GGA), as parameterized by Perdew, Burke, and Ernzerhof (PBE), predicted (0/−) values below the experimental results in Table II whereas the HSE hybrid functional gave values considerably above the experimental results.[54] Recently, Falletta and Pasquarello[55] described methods that address the many-body self-interaction when using DFT methods to model small polarons.

V. OPTICAL QUENCHING

After increasing the concentration of Ni^{3+} ions with near-band-edge 275 nm light (as shown in Fig. 3), optical quenching of the photoinduced Ni^{3+} ions was explored. Specifically, a search was made to find what wavelengths, if any, would return the Ni^{3+} EPR signal to its initial lower intensity (i.e., convert the photoinduced Ni^{3+} ions back to Ni^{2+} ions). Exposure at room temperature to longer wavelengths (940, 850, 700, 633, and 594 nm) did not decrease the Ni^{3+} EPR signal (monitored at 100 K), whereas shorter wavelengths (532 and 470 nm) brought the Ni^{3+} EPR signal close to its initial intensity. This indicates a threshold for optical quenching of the photoinduced Ni^{3+} ions near 2.2 eV. These results suggest that the primary optical quenching mechanism is the excitation of electrons from Ir^{3+} ions to the conduction band[8] with their subsequent trapping at Ni^{3+} ions to form Ni^{2+} ions. [Note: The 2.2 eV threshold was also observed in similar experiments when we directly monitored the recovery of the infrared absorption signal from the Ir^{4+} ions.] The excitation of electrons from the valence band directly to Ni^{3+} ions with photons having energies near 1.4 eV is less probable, presumably because of a small optical cross section for this process.

VI. PHOTOINDUCED OPTICAL ABSORPTION

Optical absorption spectra were obtained at room temperature from the Ni-doped β-Ga_2O_3 crystal. Figure 5(a) shows the absorption curves taken before and immediately after an exposure at room temperature to 275 nm light. In these experiments, unpolarized light from the spectrophotometer propagated along the *a* direction and the optical path length (i.e., the thickness of the crystal) was 0.84 mm. The ultraviolet light produced an increase in absorption for wavelengths in the region between 550 and 280 nm. Figure 5(b) is the difference spectrum ("after light" minus "before light"). Two broad photoinduced bands are present, peaking near 2.81 (442 nm)

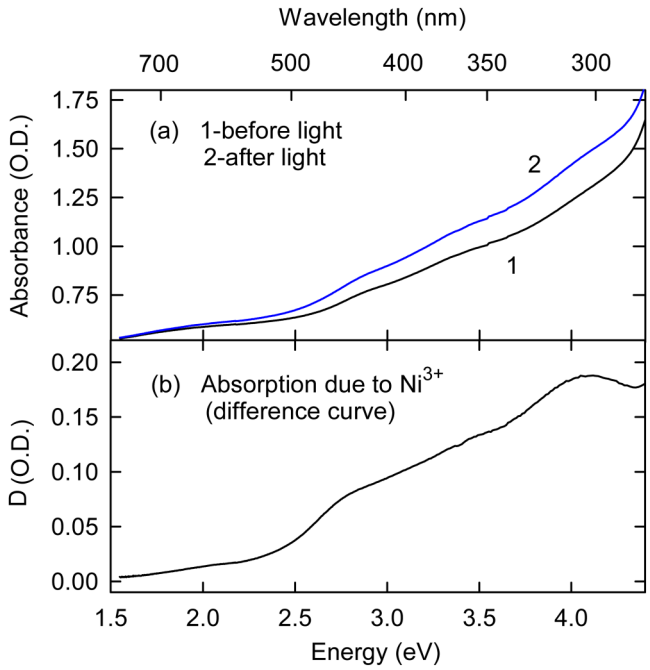

FIG. 5. Optical absorption spectra from a Ni-doped β-Ga_2O_3 crystal, taken at room temperature with unpolarized light propagating along the *a* direction in the crystal. (a) Spectrum 1 was taken before exposure to 275 nm light, and spectrum 2 was taken after exposure to 275 nm light. (b) Difference spectrum ("after light" minus "before light") showing absorption bands due to Ni^{3+} acceptors.

and 4.09 eV (303 nm). We suggest that these two absorption features in Fig. 5(b) are the expected charge-transfer bands of the Ni^{3+} ions. Their appearance in the difference spectrum is consistent with the light-induced increase in the intensity of the Ni^{3+} EPR signal (see Fig. 3). They correspond to the 3.10 (400 nm) and 4.43 eV (280 nm) absorption bands assigned to Ni^{3+} ions in α-Al_2O_3 crystals.[33,34] Additional support comes from $Y_3Al_5O_{15}$ (YAG) crystals where a charge-transfer band from Ni^{3+} ions appears at 420 nm.[56] Although expected to be weak for the concentration of Ni^{3+} encountered in our β-Ga_2O_3 crystal, absorption bands due to ^2E to ^2T internal transitions of the Ni^{3+} ions may be present in the 2.5–4.5 eV region.[57]

Additional defects are also contributing to the optical absorption spectra in Fig. 5(a). Spectrum 1 (before light) is expected to have broad absorption bands peaking near 428 and 356 nm from Ir^{4+} ions[23,36,58] and a broad absorption band peaking near 370 nm from Ni^{2+} ions. Support for this latter assertion comes from the report by Galazka *et al.*[59] of a broad optical absorption band peaking near 370 nm in an as-grown β-Ga_2O_3 crystal doped with Ni^{2+} ions. In α-Al_2O_3 crystals, a Ni^{2+} absorption band peaks near 400 nm.[33] In spectrum 1, these bands from Ir^{4+}, Ni^{2+}, and the initially present Ni^{3+} ions combine to produce a steadily increasing absorption as the band edge is approached (charge-transfer bands from Fe^{3+} ions may also be present). The absorption features associated with the Ir^{4+} and Ni^{2+} ions in spectrum 1 decrease in

intensity when the crystal is exposed to the 275 nm light and the Ni^{3+} bands grow and become more prominent. In spectrum 2 (after light) and, thus, in the difference spectrum in Fig. 5(b), there are small unresolved contributions from photoinduced Cu^{3+} bands peaking between 500 and 350 nm, as EPR shows that unintentional Cu is present in our Ni-doped crystal.[23]

VII. SUMMARY

Electron paramagnetic resonance (EPR) and optical absorption have been used to identify and characterize neutral Ni^{3+} ($3d^7$) acceptors in a β-Ga_2O_3 crystal grown by the Czochralski method. These ions have a low-spin S = 1/2 ground state. A g matrix (with principal values near 2.2) is extracted from the angular dependence of their EPR spectrum. Charge-transfer bands of the Ni^{3+} ions peak near 303 and 442 nm. At room temperature, 275 nm light moves electrons from singly ionized Ni^{2+} ($3d^8$) acceptors to singly ionized Ir^{4+} ($5d^5$) donors. Subsequent heating above 375 °C restores the initial concentration of Ni^{2+} ions when the photoinduced Ni^{3+} neutral acceptors thermally decay by hole release. This recovery temperature for the Ni^{3+} ions places the (0/−) level of the Ni acceptors in β-Ga_2O_3 at approximately 1.40 eV above the maximum of the valence band.

ACKNOWLEDGMENTS

T.D.G. was supported at the Air Force Institute of Technology by a Research Associateship Award from the National Research Council. Work at Washington State University was supported by the Air Force Office of Scientific Research under Award No. FA9550-21-1-0507 monitored by Dr. Ali Sayir. Any opinions, findings, and conclusions or recommendations expressed in this paper are those of the authors and do not necessarily reflect the views of the United States Air Force.

AUTHOR DECLARATIONS

Conflict of Interest

The authors have no conflicts to disclose.

Author Contributions

T. D. Gustafson: Conceptualization (equal); Data curation (equal); Formal analysis (equal); Investigation (equal); Writing – review & editing (equal). **N. C. Giles:** Conceptualization (equal); Funding acquisition (equal); Investigation (equal); Resources (equal); Visualization (equal); Writing – review & editing (equal). **B. C. Holloway:** Conceptualization (equal); Investigation (supporting); Writing – review & editing (equal). **J. Jesenovec:** Conceptualization (equal); Investigation (equal); Writing – review & editing (equal). **B. L. Dutton:** Conceptualization (equal); Investigation (equal); Writing – review & editing (equal). **J. S. McCloy:** Conceptualization (equal); Funding acquisition (equal); Resources (equal); Writing – review & editing (equal). **M. D. McCluskey:** Conceptualization (equal); Funding acquisition (equal); Resources (equal); Writing – review & editing (equal). **L. E. Halliburton:** Conceptualization (equal); Formal analysis (equal); Writing – original draft (lead); Writing – review & editing (equal).

DATA AVAILABILITY

The data that support the findings of this study are available within the article.

REFERENCES

[1]M. E. Ingebrigtsen, J. B. Varley, A. Y. Kuznetsov, B. G. Svensson, G. Alfieri, A. Mihaila, U. Badstübner, and L. Vines, "Iron and intrinsic deep level states in Ga_2O_3," Appl. Phys. Lett. **112**, 042104 (2018).
[2]A. Y. Polyakov, N. B. Smirnov, I. V. Shchemerov, S. J. Pearton, F. Ren, A. V. Chernykh, and A. I. Kochkova, "Electrical properties of bulk semi-insulating β-Ga_2O_3 (Fe)," Appl. Phys. Lett. **113**, 142102 (2018).
[3]A. Y. Polyakov, N. B. Smirnov, I. V. Schemerov, A. V. Chernykh, E. B. Yakimov, A. I. Kochkova, A. N. Tereshchenko, and S. J. Pearton, "Electrical properties, deep levels and luminescence related to Fe in bulk semi-insulating β-Ga_2O_3 doped with Fe," ECS J. Solid State Sci. Technol. **8**, Q3091 (2019).
[4]A. Mauze, Y. Zhang, T. Mates, F. Wu, and J. S. Speck, "Investigation of unintentional Fe incorporation in (010) β-Ga_2O_3 films grown by plasma-assisted molecular beam epitaxy," Appl. Phys. Lett. **115**, 052102 (2019).
[5]S. Bhandari, M. E. Zvanut, and J. B. Varley, "Optical absorption of Fe in doped Ga_2O_3," J. Appl. Phys. **126**, 165703 (2019).
[6]C. A. Lenyk, T. D. Gustafson, L. E. Halliburton, and N. C. Giles, "Deep donors and acceptors in β-Ga_2O_3 crystals: Determination of the $Fe^{2+/3+}$ level by a non-contact method," J. Appl. Phys. **126**, 245701 (2019).
[7]C. Zimmermann, Y. K. Frodason, A. W. Barnard, J. B. Varley, K. Irmscher, Z. Galazka, A. Karjalainen, W. E. Meyer, F. D. Auret, and L. Vines, "Ti- and Fe-related charge transition levels in β-Ga_2O_3," Appl. Phys. Lett. **116**, 072101 (2020).
[8]S. Bhandari and M. E. Zvanut, "Optical transitions for impurities in Ga_2O_3 as determined by photo-induced electron paramagnetic resonance spectroscopy," J. Appl. Phys. **127**, 065704 (2020).
[9]A. Y. Polyakov, I.-H. Lee, A. Miakonkikh, A. V. Chernykh, N. B. Smirnov, I. V. Shchemerov, A. I. Kochkova, A. A. Vasilev, and S. J. Pearton, "Anisotropy of hydrogen plasma effects in bulk n-type β-Ga_2O_3," J. Appl. Phys. **127**, 175702 (2020).
[10]T. D. Gustafson, C. A. Lenyk, L. E. Halliburton, and N. C. Giles, "Deep donor behavior of iron in β-Ga_2O_3 crystals: Establishing the $Fe^{4+/3+}$ level," J. Appl. Phys. **128**, 145704 (2020).
[11]S. Bhandari and M. E. Zvanut, "Charge trapping at Fe due to midgap levels in Ga_2O_3," J. Appl. Phys. **129**, 085703 (2021).
[12]S. Bhandari and M. E. Zvanut, "Fe-related optical transitions in floating zone and Czochralski grown β-Ga_2O_3 crystals," J. Appl. Phys. **130**, 165701 (2021).
[13]H. H. Tippins, "Optical and microwave properties of trivalent chromium in β-Ga_2O_3," Phys. Rev. **137**, A865 (1965).
[14]C. G. Walsh, J. F. Donegan, T. J. Glynn, G. P. Morgan, G. F. Imbusch, and J. P. Remeika, "Luminescence from β-Ga_2O_3:Cr^{3+}," J. Lumin. **40-41**, 103 (1988).
[15]A. Luchechko, V. Vasyltsiv, Y. Zhydachevskyy, M. Kushlyk, S. Ubizskii, and A. Suchocki, "Luminescence spectroscopy of Cr^{3+} ions in bulk single crystalline β-Ga_2O_3," J. Phys. D: Appl. Phys. **53**, 354001 (2020).
[16]A. Luchechko, V. Vasyltsiv, L. Kostyk, O. Tsvetkova, and B. Pavlyk, "The effect of Cr^{3+} and Mg^{2+} impurities on thermoluminescence and deep traps in β-Ga_2O_3 crystals," ECS J. Solid State Sci. Technol. **9**, 045008 (2020).
[17]R. Sun, Y. K. Ooi, P. T. Dickens, K. G. Lynn, and M. A. Scarpulla, "On the origin of red luminescence from iron-doped β-Ga_2O_3 bulk crystals," Appl. Phys. Lett. **117**, 052101 (2020).
[18]J. E. Stehr, M. Jansson, D. M. Hofmann, J. Kim, S. J. Pearton, W. M. Chen, and I. A. Buyanova, "Magneto-optical properties of Cr^{3+} in β-Ga_2O_3," Appl. Phys. Lett. **119**, 052101 (2021).
[19]V. Vasyltsiv, A. Luchechko, Y. Zhydachevskyy, L. Kostyk, R. Lys, D. Slobodzyan, R. Jakieła, B. Pavlyk, and A. Suchocki, "Correlation between electrical conductivity and luminescence properties in β-Ga_2O_3:Cr^{3+} and β-Ga_2O_3:Cr,Mg single crystals," J. Vac. Sci. Technol., A **39**, 033201 (2021).

[20]C. Remple, J. Huso, and M. D. McCluskey, "Photoluminescence and Raman mapping of β-Ga_2O_3," AIP Adv. **11**, 105006 (2021).
[21]M. Peres, D. M. Esteves, B. M. S. Teixeira, J. Zanoni, L. C. Alves, E. Alves, L. F. Santos, X. Biquard, Z. Jia, W. Mu, J. Rodrigues, N. A. Sobolev, M. R. Correia, T. Monteiro, N. Ben Sedrine, and K. Lorenz, "Enhancing the luminescence yield of Cr^{3+} in β-Ga_2O_3 by proton irradiation," Appl. Phys. Lett. **120**, 261904 (2022).
[22]J. Jesenovec, C. Pansegrau, M. D. McCluskey, J. S. McCloy, T. D. Gustafson, L. E. Halliburton, and J. B. Varley, "Persistent room-temperature photodarkening in Cu-doped β-Ga_2O_3," Phys. Rev. Lett. **128**, 077402 (2022).
[23]T. D. Gustafson, N. C. Giles, B. C. Holloway, C. A. Lenyk, J. Jesenovec, J. S. McCloy, M. D. McCluskey, and L. E. Halliburton, "Cu^{2+} and Cu^{3+} acceptors in β-Ga_2O_3 crystals: A magnetic resonance and optical absorption study," J. Appl. Phys. **131**, 065702 (2022).
[24]J. Jesenovec, C. Remple, J. Huso, B. Dutton, P. Toews, M. D. McCluskey, and J. S. McCloy, "Photodarkening and dopant segregation in Cu-doped β-Ga_2O_3 Czochralski single crystals," J. Cryst. Growth **578**, 126419 (2022).
[25]F. Mentink-Vigier, L. Binet, G. Vignoles, D. Gourier, and H. Vezin, "Giant titanium electron wave function in gallium oxide: A potential electron-nuclear spin system for quantum information processing," Phys. Rev. B **82**, 184414 (2010).
[26]I. G. Kim, T. H. Yeom, S. H. Lee, Y. M. Yu, H. W. Shin, and S. H. Choh, "Electron paramagnetic resonance studies of Mn^{2+} ions in β-Ga_2O_3 single crystal," J. Appl. Phys. **89**, 4470 (2001).
[27]J. E. Stehr, D. M. Hofmann, J. Schörmann, M. Becker, W. M. Chen, and I. A. Buyanova, "Electron paramagnetic resonance signatures of Co^{2+} and Cu^{2+} in β-Ga_2O_3," Appl. Phys. Lett. **115**, 242101 (2019).
[28]S. Geschwind and J. P. Remeika, "Spin resonance of transition metal ions in corundum," J. Appl. Phys. **33**, 370 (1962).
[29]W.-Z. Xiao, L.-L. Wang, L. Xu, Q. Wan, and B. S. Zou, "Electronic structure and magnetic interactions in Ni-doped β-Ga_2O_3 from first-principles calculations," Scr. Mater. **61**, 477 (2009).
[30]M. Labed, N. Sengouga, M. Labed, A. Meftah, S. Kyoung, H. Kim, and Y. S. Rim, "Modeling a Ni/β-Ga_2O_3 Schottky barrier diode deposited by confined magnetic-field-based sputtering," J. Phys. D: Appl. Phys. **54**, 115102 (2021).
[31]Y.-H. Hong, X.-F. Zheng, Y.-L. He, F. Zhang, X.-Y. Zhang, X.-C. Wang, J.-N. Li, D.-P. Wang, X.-L. Lu, H.-B. Han, X.-H. Ma, and Y. Hao, "The optimized interface characteristics of β-Ga_2O_3 Schottky barrier diode with low temperature annealing," Appl. Phys. Lett. **119**, 132103 (2021).
[32]L. N. Shen and T. L. Estle, "An investigation of the nature of the Jahn-Teller effect for Ni^{3+} in Al_2O_3 by electron paramagnetic resonance," J. Phys. C: Solid State Phys. **12**, 2103 (1979).
[33]R. Müller and H. H. Günthard, "Spectroscopic study of the reduction of nickel and cobalt ions in sapphire," J. Chem. Phys. **44**, 365 (1966).
[34]H. H. Tippins, "Charge-transfer spectra of transition-metal ions in corundum," Phys. Rev. B **1**, 126 (1970).
[35]S. A. Marshall, T. T. Kikuchi, and A. R. Reinberg, "Paramagnetic resonance absorption of divalent nickel in α-Al_2O_3 single crystal," Phys. Rev. **125**, 453 (1962).
[36]J. Jesenovec, J. Varley, S. E. Karcher, and J. S. McCloy, "Electronic and optical properties of Zn-doped β-Ga_2O_3 Czochralski single crystals," J. Appl. Phys. **129**, 225702 (2021).
[37]J. S. McCloy, J. Jesenovec, B. L. Dutton, C. Pansegrau, C. Remple, M. H. Weber, S. Swain, M. McCluskey, and M. Scarpulla, "Growth and defect characterization of doped and undoped β-Ga_2O_3 crystals," Proc. SPIE **12002**, 1200205 (2022).
[38]J. Jesenovec, "Doping and alloying of monoclinic β-Ga_2O_3 grown by Czochralski and vertical gradient freeze," Ph.D. dissertation (Washington State University, Pullman, WA, 2022), available at ProQuest Dissertations and Theses.
[39]S. Geller, "Crystal structure of β-Ga_2O_3," J. Chem. Phys. **33**, 676 (1960).
[40]J. Åhman, G. Svensson, and J. Albertsson, "A reinvestigation of β-gallium oxide," Acta Crystallogr., Sect. C: Cryst. Struct. Commun. **52**, 1336 (1996).
[41]T. D. Gustafson, J. Jesenovec, C. A. Lenyk, N. C. Giles, J. S. McCloy, M. D. McCluskey, and L. E. Halliburton, "Zn acceptors in β-Ga_2O_3 crystals," J. Appl. Phys. **129**, 155701 (2021).
[42]R. D. Shannon, "Revised effective ionic radii and systematic studies of interatomic distances in halides and chalcogenides," Acta Crystallogr., Sect. A **32**, 751 (1976).
[43]C. A. Lenyk, N. C. Giles, E. M. Scherrer, B. E. Kananen, L. E. Halliburton, K. T. Stevens, G. K. Foundos, J. D. Blevins, D. L. Dorsey, and S. Mou, "Ir^{4+} ions in β-Ga_2O_3 crystals: An unintentional deep donor," J. Appl. Phys. **125**, 045703 (2019).
[44]M. L. Meil'man, "EPR of Fe^{3+} ions in β-Ga_2O_3 crystals," Sov. Phys. Solid State **11**, 1403 (1969).
[45]J. R. Ritter, K. G. Lynn, and M. D. McCluskey, "Iridium-related complexes in Czochralski-grown β-Ga_2O_3," J. Appl. Phys. **126**, 225705 (2019).
[46]J. T. Randall and M. H. F. Wilkins, "Phosphorescence and electron traps. I. The study of trap distributions," Proc. R. Soc. London, Ser. A **184**, 366 (1945).
[47]A. G. Milnes, *Deep Impurities in Semiconductors* (John Wiley and Sons, New York, 1973), Chap. 9, pp. 227–228.
[48]B. E. Kananen, L. E. Halliburton, E. M. Scherrer, K. T. Stevens, G. K. Foundos, K. B. Chang, and N. C. Giles, "Electron paramagnetic resonance study of neutral Mg acceptors in β-Ga_2O_3 crystals," Appl. Phys. Lett. **111**, 072102 (2017).
[49]Q. D. Ho, T. Frauenheim, and P. Deák, "Theoretical confirmation of the polaron model for the Mg acceptor in β-Ga_2O_3," J. Appl. Phys. **124**, 145702 (2018).
[50]D. Skachkov and W. R. L. Lambrecht, "Computational study of electron paramagnetic resonance parameters for Mg and Zn impurities in β-Ga_2O_3," Appl. Phys. Lett. **114**, 202102 (2019).
[51]C. A. Lenyk, T. D. Gustafson, S. A. Basun, L. E. Halliburton, and N. C. Giles, "Experimental determination of the (0/−) level for Mg acceptors in β-Ga_2O_3 crystals," Appl. Phys. Lett. **116**, 142101 (2020).
[52]E. Chikoidze, C. Sartel, H. Yamano, Z. Chi, G. Bouchez, F. Jomard, V. Sallet, G. Guillot, K. Boukheddaden, A. Pérez-Tomás, T. Tchelidze, and Y. Dumont, "Electrical properties of *p*-type Zn:Ga_2O_3 thin films," J. Vac. Sci. Technol., A **40**, 043401 (2022).
[53]Q. D. Ho, D. K. Nguyen, and H. A. Huy, "Computational study of hyperfine interaction for Zn substitute Ga in β-Ga_2O_3," Comput. Condens. Matter **32**, e00727 (2022).
[54]A. Kyrtsos, M. Matsubara, and E. Bellotti, "On the feasibility of p-type Ga_2O_3," Appl. Phys. Lett. **112**, 032108 (2018).
[55]S. Falletta and A. Pasquarello, "Polarons free from many-body self-interaction in density functional theory," Phys. Rev. B **106**, 125119 (2022).
[56]S. R. Rotman, M. Roth, H. L. Tuller, and C. Warde, "Defect-property correlations in garnet crystals.: IV. The optical properties of nickel-doped yttrium aluminum garnet," J. Appl. Phys. **66**, 1366 (1989).
[57]M. N. Sanz-Ortiz, F. Rodríguez, J. Rodríguez, and G. Demazeau, "Optical and magnetic characterisation of Co^{3+} and Ni^{3+} in $LaAlO_3$: Interplay between the spin state and Jahn-Teller effect," J. Phys.: Condens. Matter **23**, 415501 (2011).
[58]J. R. Ritter, J. Huso, P. T. Dickens, J. B. Varley, K. G. Lynn, and M. D. McCluskey, "Compensation and hydrogen passivation of magnesium acceptors in β-Ga_2O_3," Appl. Phys. Lett. **113**, 052101 (2018).
[59]Z. Galazka, K. Irmscher, R. Schewski, I. M. Hanke, M. Pietsch, S. Ganschow, D. Klimm, A. Dittmar, A. Fiedler, T. Schroeder, and M. Bickermann, "Czochralski-grown bulk β-Ga_2O_3 single crystals doped with mono-, di-, tri-, and tetravalent ions," J. Cryst. Growth **529**, 125297 (2020).